

This work was written as part of one of the author's official duties as an Employee of the United States Government and is therefore a work of the United States Government. In accordance with 17 U.S.C. 105, no copyright protection is available for such works under U.S. Law. Access to this work was provided by the University of Maryland, Baltimore County (UMBC) ScholarWorks@UMBC digital repository on the Maryland Shared Open Access (MD-SOAR) platform.

Please provide feedback

Please support the ScholarWorks@UMBC repository by emailing [scholarworks-group@umbc.edu](mailto:scholarworks-group@umbc.edu) and telling us what having access to this work means to you and why it's important to you. Thank you.

N. MATTIUCCI<sup>1,2,3</sup>  
 G. D'AGUANNO<sup>1,2,✉</sup>  
 M. SCALORA<sup>2</sup>  
 M. J. BLOEMER<sup>2</sup>

# Cross-phase modulation in one-dimensional photonic crystals: applications to all-optical devices

<sup>1</sup>Time Domain Corporation, Cummings Research Park, 7097 Old Madison Pike, Huntsville, AL 35806, USA

<sup>2</sup>Charles M. Bowden Research Center, RDECOM Bldg 7804, Redstone Arsenal, AL 35898-5000, USA

<sup>3</sup>Università 'RomaTre', Dipartimento di Fisica 'E. Amaldi', Via Della Vasca Navale 84, 00146 Rome, Italy

Received: 16 March 2005

Published online: 2 June 2005 • © Springer-Verlag 2005

**ABSTRACT** We present a numerical study of a finite photonic band gap structure with a  $\chi^{(3)}$  nonlinearity that couples two input pump beams at frequencies  $\omega_1$  and  $\omega_2$ . We show that in this configuration a variety of all-optical devices can be obtained: an optical transistor, a double switch, and a dynamical switch.

PACS 42.65.-k; 42.65.Pc; 42.79.-e

## 1 Introduction

The seminal work of Chen and Mills [1] on the appearance of gap solitons in one-dimensional photonic crystals (1-D PCs) with a  $\chi^{(3)}$  nonlinearity can be characterized as the beginning of a period of intense experimental and theoretical investigations whose focus was to study the possibility of using these structures as all-optical devices: as switching and limiting devices, and as diodes [2–8]. Although a large number of papers have already been published on the subject, the vast majority of them generally consider configurations with only one input pump beam, limiting the flexibility of the proposed devices. In Ref. [8] a more flexible configuration was studied, but the proposed device is an electro-optic rather than an all-optical device. Here we study an all-optical device based on a two-pump scheme, where the two pumps are coupled by the cross phase modulation terms of the cubic nonlinearity. In particular, we will discuss an optical transistor, a double switch, and a dynamical switch. The paper is organized as follows: in Sect. 2 we briefly discuss the mathematical model and the characteristics of the PC structure used for the simulations; Sect. 3 is devoted to the optical transistor and the double switch; finally in Sect. 4 we study the dynamical switch.

## 2 The model

Our study is based on the plane monochromatic wave approach. Two input beams, of frequencies  $\omega_1$  and  $\omega_2$ ,

respectively, propagate in the  $z$  direction and arrive at normal incidence at the input surface of a 1-D PC composed of alternating layers of a linear dielectric material juxtaposed to a nonlinear dielectric material with a cubic nonlinearity. The two waves are assumed to be linearly polarized in the same direction. The problem can be described by the following system of nonlinear coupled differential equations:

$$\begin{cases} \frac{d^2 E_1}{dz^2} + \frac{\omega_1^2}{c^2} [n_1(z) + 3\sigma_{11}(z)|E_1|^2 + 6\sigma_{21}(z)|E_2|^2] \\ \quad \times E_1 = 0, \\ \frac{d^2 E_2}{dz^2} + \frac{\omega_2^2}{c^2} [n_2(z) + 3\sigma_{22}(z)|E_2|^2 + 6\sigma_{12}(z)|E_1|^2] \\ \quad \times E_2 = 0, \end{cases} \quad (1)$$

where  $E_1$  and  $E_2$  are the amplitudes of the electric fields, normalized with respect to the input amplitudes, at frequencies  $\omega_1$  and  $\omega_2$ , respectively. The dimensionless coefficients  $\sigma$  are the elements of the  $\chi^{(3)}$  tensor multiplied by the square modulus of the related input amplitudes (i.e.  $\sigma_i(\omega_j) = \chi^{(3)}(\omega_i, \omega_i, \omega_j)|E_i^{(0)}|^2$ ). For simplicity, we assume that the  $\chi^{(3)}$  tensor is not dispersive, so that  $\sigma_{11} = \sigma_{12} = \sigma_1$  and  $\sigma_{21} = \sigma_{22} = \sigma_2$ .  $n_1$  and  $n_2$  are the  $z$ -dependent, linear refractive indices, at frequencies  $\omega_1$  and  $\omega_2$ , respectively. We consider a 1-D PC composed of  $N = 40$  periods, and we assume that the elementary cell is made of two layers of non-dispersive and non-absorbing dielectric materials of low refractive index  $n_L = 1.7$ ,  $\lambda/4n_L$  thick, and high refractive index  $n_H = 3.5$ ,  $\lambda/2n_H$  thick, respectively. The reference wavelength is  $\lambda = 1 \mu\text{m}$ . The low-index layer exhibits the  $\chi^{(3)}$  nonlinearity.

In Fig. 1 we show the linear transmission ( $T$ ) of the structure. The arrows indicate the tuning of the two incident pumps. The  $\omega_1$  pump is tuned at the low frequency band edge transmission resonance, while the  $\omega_2$  pump is tuned at the high frequency band edge transmission resonance. In both cases  $T \sim 1$ . We note that this structure was not optimized for the devices that will be studied in the next sections. So, we seek proof-of-principle results and an understanding of the qualitative aspects of the dynamics that ensues when two pumps are coupled as in Eq. (1) above. Moreover, although in our calculations we use a  $\lambda/4-\lambda/2$  structure, similar results can be expected for different types of structures. We numerically

✉ Fax: +1-256-9557216, E-mail: giuseppe.daguanno@timedomain.com

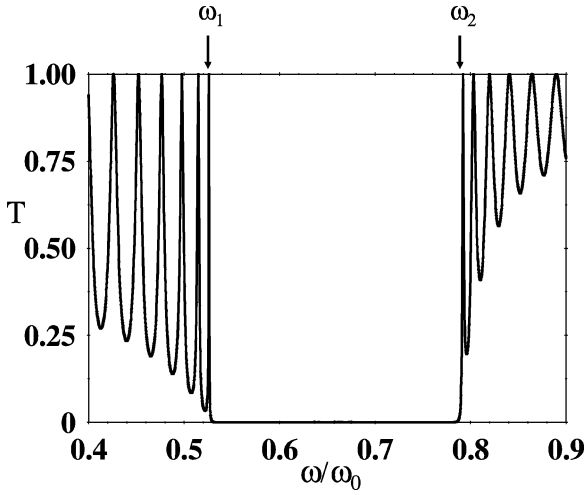


**FIGURE 1** Linear transmission vs.  $\omega/\omega_0$ , where  $\lambda_0 = 1 \mu\text{m}$  is the reference wavelength and  $\omega_0 = 2\pi c/\lambda_0$ . The structure is composed of  $N = 40$  periods. The elementary cell consists of two layers of refractive indices  $n_H = 3.5$  and  $n_L = 1.7$ , respectively. The thicknesses of the two layers are respectively  $d_H = \lambda_0/2n_H$  and  $d_L = \lambda_0/4n_L$ . The structure is surrounded by air ( $n_0 = 1$ ). The arrows indicate the positions of the two pumps ( $\omega_1$  and  $\omega_2$ ) on the transmission spectrum

integrate Eq. (1) using a shooting procedure, as described in Refs. [9, 10], for example.

### 3 Optical transistor and double switch

In electronics, a transistor is made of three layers of a doped semiconductor material. The three-layer structure consists of an n-type (p-type) semiconductor layer sandwiched between two p-type (n-type) layers. In such a device a small change in the current or voltage at the inner semiconductor layer, which acts as control, produces a large change in the current passing through the entire structure. The device can thus act as a switch, opening and closing an electronic gate. From this point of view, the optical configuration we propose shows transistor-like behavior. In Fig. 2 we show that a small change in the intensity of the  $\omega_2$  pump produces a large change in the transmitted intensity of the  $\omega_1$  field (dashed line), a behavior that is due to the optical bistability induced by the  $\omega_2$  pump. In fact, if we turn off the electric field  $E_2$  and allow the intensity of the  $\omega_1$  pump to vary, no bistable behavior is noted (Fig. 2, solid line). The  $\omega_2$  pump also manifests bistable behavior, as shown in Fig. 3. The device can then be used as a double switch, as the switching point of the transmitted fields at  $\omega_1$  and  $\omega_2$  is the same for both curves. In Figs. 4 and 5 we show the square moduli of  $E_1$  and  $E_2$ , respectively, inside the PC before the switch (thin solid line), when  $\sigma_1 = 0.002$  and  $\sigma_2 = 0.002$ , and after the switch (thick solid line), when  $\sigma_1 = 0.002$  and  $\sigma_2 = 0.03$ . Note that for  $\sigma_1 = 0.002$  the nonlinear transmission for  $\omega_1$  is  $T \sim 0.75$ , and  $E_1$  has the characteristic bell-shaped envelope consistent with its tuning very near the peak of transmission of the low frequency band edge [11], close to its original tuning position. This clearly indicates that the transmission resonance for the  $\omega_1$  pump has suffered a small, nonlinear shift toward low frequencies. On the other hand, for the same control parameter (i.e.  $\sigma_2 = \sigma_1 = 0.002$ ), the high frequency band edge transmission resonance has already suffered a large

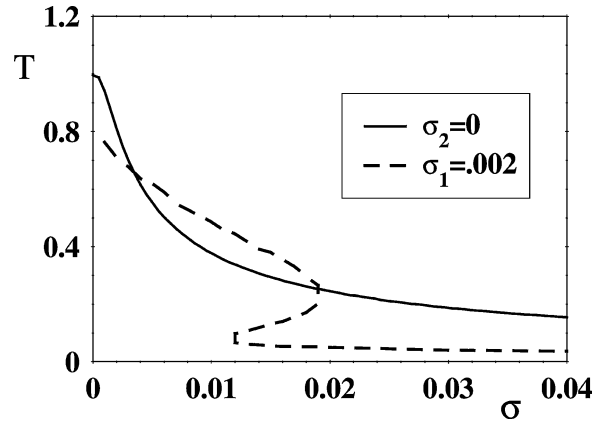


**FIGURE 2** Nonlinear transmission of the electric field  $E_1$ . The solid line is the transmission of the electric field  $E_1$  as a function of its own control parameter  $\sigma_1 = \chi^{(3)}|E_1^{(0)}|^2$  (the second pump  $\omega_2$  is in this case turned off: i.e.  $\sigma_2 = 0$ ).  $E_j^{(0)}$ , with  $j = 1, 2$ , are the amplitudes of the input fields at frequencies  $\omega_1$  and  $\omega_2$ , respectively. The dashed line is the transmission of the electric field  $E_1$  as a function of the control parameter  $g\sigma_y = \chi^{(3)}|E_2^{(0)}|^2$  (the first pump  $\omega_1$  is in this case set at a fixed value:  $\sigma_1 = 0.002$ ). In the first case (solid line) in the abscissa axis  $\sigma$  stays for  $\sigma_1$  while in the second case (dashed line)  $\sigma$  stays for  $\sigma_2$

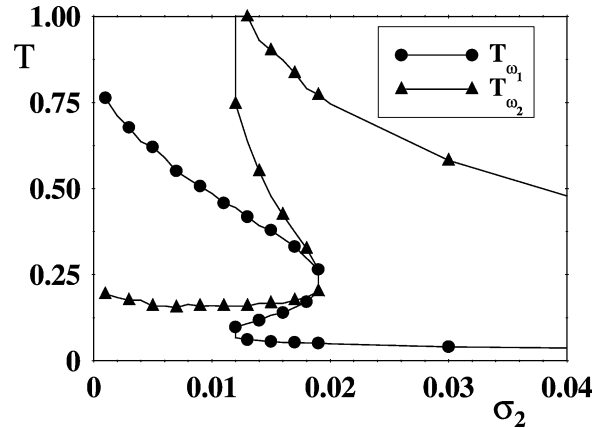


**FIGURE 3** Transmission of the electric fields  $E_1$  and  $E_2$  vs.  $\sigma_2$ . The control parameter of the first pump is set at  $\sigma_1 = 0.002$

shift toward low frequencies causing the  $E_2$  field to ‘fall’ in the valley between the first and the second transmission resonances, at the high-frequency band edge, with  $T \sim 0.25$ . The different behavior of the two fields can be easily explained because of their different localization properties within the PC:  $E_1$  is initially mostly localized in the linear, high-index layers, while  $E_2$  is initially localized in the nonlinear, low-index, layers. After switching occurs, the nonlinear shift of the transmission causes the  $E_1$  field to fall inside the gap, near the low-frequency band edge. The  $E_2$  field is then tuned near the second peak of transmission of the high-frequency band edge, consistent with its double-bell-shaped envelope.

### 4 Dynamical switch

A simple all-optical switch in PC structures with a cubic nonlinearity has been studied in Refs. [3, 4]. In the present case, our device can benefit from additional flexibility by dynamically (or parametrically) controlling the switching

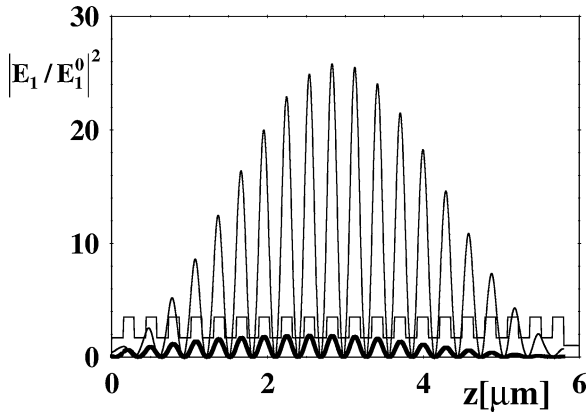


**FIGURE 4** Square modulus of  $E_1/E_1^{(0)}$  inside the structure. The *thick solid line* represents the field profile after the switching ( $\sigma_1 = 0.002$  and  $\sigma_2 = 0.03$ ). The *thin solid line* represents the field profile before the switching ( $\sigma_1 = 0.002$  and  $\sigma_2 = 0.002$ )

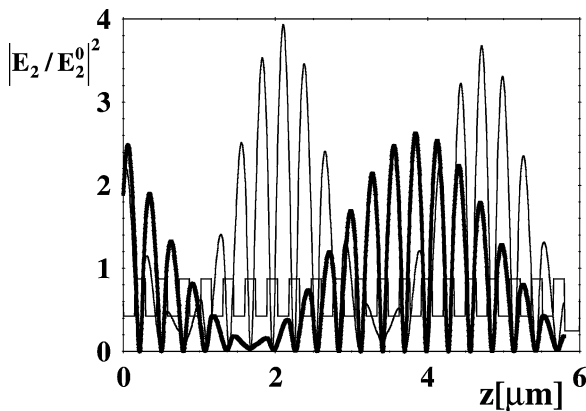


**FIGURE 5** Square modulus of  $E_2/E_2^{(0)}$  inside the structure after the switching (*thick solid line*) for  $\sigma_1 = 0.002$  and  $\sigma_2 = 0.03$  and before the switching (*thin solid line*) for  $\sigma_1 = 0.002$  and  $\sigma_2 = 0.002$

point of the  $E_2$  field using the intensity of the  $E_1$  field. In other words, we fix the intensity of the  $E_1$  input field, vary the intensity of the  $E_2$  field, and so monitor the change of the switching point of the  $E_2$  field for different values of the  $E_1$  intensity. In Fig. 6 we calculate the nonlinear transmission curves of the  $E_2$  field vs.  $\sigma_2$  for different values

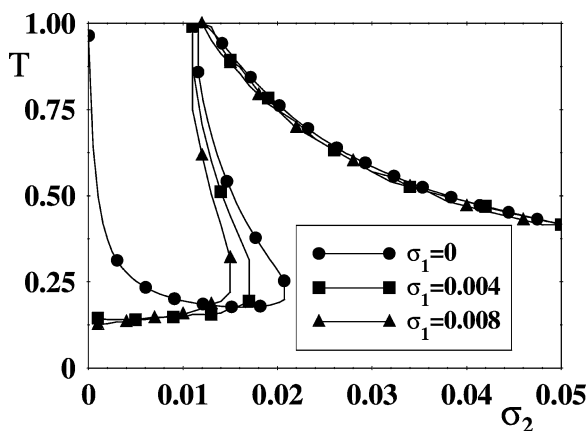


**FIGURE 6** Transmission of the electric field  $E_2$  vs.  $\sigma_2$  for different values of the control parameter  $\sigma_1$

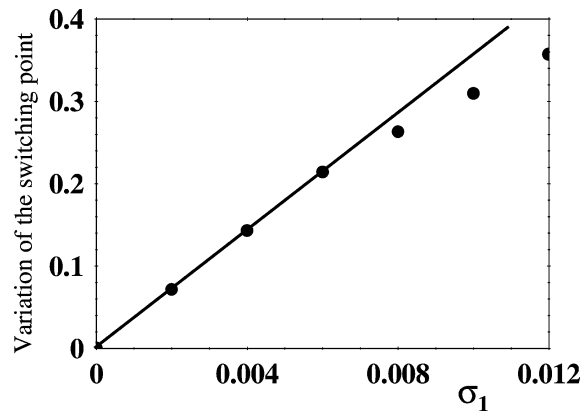


**FIGURE 7** Variation of the switching point of the  $E_2$  field vs.  $\sigma_1$ . The switching point is indicated as  $\sigma_{2s}$  and the relative variation of the switching point is calculated as follows:  $(\sigma_{2s}(\sigma_1 = 0) - \sigma_{2s}(\sigma_1))/\sigma_{2s}(\sigma_1 = 0)$ . The *circles* represent the actual calculated data. The *straight, solid line* connecting the first points indicates that the variation of the switching point is linear only for small values of the control parameter  $\sigma_1$ . In this case saturation effects come into play above  $\sigma_1 \sim 0.006$

of the parameter  $\sigma_1$  ( $\sigma_1 = 0; 0.004; 0.008$ ). The figure shows that the switching point is reached for lower values of  $\sigma_2$  as  $\sigma_1$  increases. In other words, the larger the intensity of the  $\omega_x$  pump, the lower the intensity of the  $\omega_2$  pump will be to achieve self-switching. In Fig. 7 we show the variation of the switching point ( $\sigma_{2s}$ ) as a function of the  $\sigma_1$  parameter. Note that while for low values of  $\sigma_1$  the curve is linear, for higher values of  $\sigma_1$  the curve shows saturating behavior.

## 5 Conclusions

In summary, we have shown that a 1-D PC doped with a  $\chi^{(3)}$  nonlinearity, and pumped with two electromagnetic fields, can act as a more versatile device compared to having just a single pump. The switching properties of the structure [3, 4, 7] can be improved by using a double-pumping scheme such that both pumps are tuned to their respective band edges, and become localized inside the stack. The dynamics that ensues gives rise to a double switch (Fig. 3) and to a dynamical switch (Fig. 6). An all-optical transistor (Fig. 2) is also envisioned.

## REFERENCES

- 1 W. Chen, D.L. Mills, Phys. Rev. Lett. **58**, 160 (1987)
- 2 J. He, M. Cada, Appl. Phys. Lett. **61**, 2150 (1992)
- 3 B. Acklin, M. Cada, J. He, M.-A. Dupertuis, Appl. Phys. Lett. **63**, 2177 (1993)
- 4 M. Scalora, J.P. Dowling, C.M. Bowden, M.J. Bloemer, Phys. Rev. Lett. **73**, 1368 (1994)
- 5 M. Scalora, J.P. Dowling, C.M. Bowden, M.J. Bloemer, J. Appl. Phys. **76**, 2023 (1994)
- 6 M.D. Tocci, M.J. Bloemer, M. Scalora, J.P. Dowling, C.M. Bowden, Appl. Phys. Lett. **66**, 2324 (1995)
- 7 S. Janz, J. He, Z.R. Wasilewski, M. Cada, Appl. Phys. Lett. **67**, 1051 (1995)
- 8 P. Xie, Z.-Q. Zhang, J. Appl. Phys. **95**, 1630 (2004)
- 9 R.S. Bennink, Y.-K. Yoon, R.W. Boyd, J.E. Sipe, Opt. Lett. **24**, 1416 (1999)
- 10 W.H. Press, B.P. Flannery, S.A. Teukolsky, W.T. Vetterling, *Numerical Recipes in C* (Cambridge University Press, Cambridge, 1988)
- 11 G. D'Aguanno, M. Centini, M. Scalora, C. Sibilia, Y. Dumeige, P. Vidakovic, J.A. Levenson, M.J. Bloemer, C.M. Bowden, J.W. Haus, M. Bertolotti, Phys. Rev. E **64**, 16609 (2001)